Contribution from the Department of Chemistry, The University of Mississippi, University, Mississippi 38677, and Fairchild Industries, Palo Alto, California

# Crystal Structure of $LiV_2F_6$, a Mixed-Valence Trirutile

R. M. METZGER,*[1a] N. E. HEIMER,[1a] C. S. KUO,[1b] R. F. WILLIAMSON,[1a] and W. O. J. BOO*[1a]

*Received August 11, 1982*

$LiV_2F_6$ crystallizes in space group $P4_2/mnm$ with lattice constants $a$ = 4.697 (3) Å, $c$ = 9.289 (3) Å, and $Z$ = 2. The structure refinement for a trirutile lattice [V at 4e, $z/c$ = 0.33263 (8); F1 at 4f, $x/a$ = 0.3094 (11); F2 at 8j, $x/a$ = 0.2971 (9), $z/c$ = 0.3277 (3)] gave $R$ = 5.0% for 371 reflections and showed two edge-sharing distorted $VF_6$ octahedra and a single V site. The compound is truly mixed-valent. The distortions of the $VF_6$ octahedra and the inferred reordering of $V^{II}$ and $V^{III}$ energy levels help to explain the temperature-dependent magnetic susceptibility of $LiV_2F_6$ (which has been remeasured). Madelung energies are also reported.

## Introduction

There has been considerable interest in the magnetic properties of the divalent fluorides of the first-row transition metals $MF_2$, most of which crystallize in the rutile ($TiO_2$) structure,[2] space group $P4_2/mnm$ ($D_{4h}^{14}$) [M = V,[3] Mn,[4] Fe,[4] Co,[4] Ni,[4] Zn[4]], and some in a distorted rutile lattice, space group $P2_1/c$ ($C_{2h}^5$) [M = Cr,[5a] Cu[5b]]. In these compounds, magnetic interactions between neighboring cations are predominantly antiferromagnetic, consistent with predictions by Goodenough[6] and Kanamori.[7] At low temperatures, two magnetically ordered structures were found in this series. In $CrF_2$,[8] $MnF_2$,[9] $FeF_2$,[9] $CoF_2$,[9] $NiF_2$,[9] and $CuF_2$,[10] a strong antiferromagnetic coupling between second nearest neighboring cations results in three-dimensional long-range ordered structures of the A–B interpenetrating sublattice type. In $VF_2$,[11] the dominating magnetic interaction (antiferromagnetic) is between nearest neighboring cations. For this reason, magnetic ordering in $VF_2$ occurs in two steps as the temperature is lowered. Below about 100 K, antiferromagnetic short-range order sets in, forming ordered linear chains parallel to the crystallographic $c$ axis.[3,11] Below 7 K, three-dimensional long-range order between neighboring chains causes them to become incommensurate spirals.[3,11]

Other rutile-type metal fluorides have been studied extensively in this laboratory,[12] and of these, $LiV_2F_6$ ($LiV^{II}V^{III}F_6$) was found to be particularly interesting. It was believed to crystallize in the trirutile (or tapiolite[13]) lattice [space group $P4_2/mnm$ ($D_{4h}^{14}$), which is also the space group for rutile]. It will be shown below that this assignment is correct. Magnetic susceptibility measurements[12] for $LiV_2F_6$ showed a behavior reminiscent of that of $VF_2$: deviation from high-temperature paramagnetic behavior occurs below 100 K, but long-range antiferromagnetic ordering occurs near 26 K. In addition to having a higher Néel temperature than $VF_2$, $LiV_2F_6$ was found to have a Curie–Weiss constant close to zero ($\Theta$ = −3 K) as opposed to $\Theta$ = −88 K for $VF_2$.[12] A new $\Theta$ value for $LiV_2F_6$ is reported below. This strongly suggests that magnetic interactions in $LiV_2F_6$ are different from those in $VF_2$. In rutile-type structures such as $VF_2$ there are only two important exchange interactions: those between nearest neighbors ($J_1$) and those between second nearest neighbors ($J_2$). As emphasized above, the preponderant interactions are strictly antiferromagnetic in $VF_2$. In contrast, the magnetic data imply that one or the other of these exchange interactions is ferromagnetic in $LiV_2F_6$.

Other fluorides of the general formula $LiM^{II}M^{III}F_6$ ($M^{II}$ = Mg, Mn, Fe, Co, Ni, Cu, or Zn; $M^{III}$ = Ti, V, Cr, Fe, or Ga) have also been reported to crystallize in the trirutile lattice.[14] No complete crystal structure determinations, however, have been reported for these salts except for the alloy $Li_{0.75}Zn_{0.25}(Zn_{1.25}Cr_{0.75})F_6$.[14e] The compound $LiV_2F_6$ is unique because the $V^{2+}$ ($d^3$) ion has not been previously studied in any other trirutile compound. The aim of this study is to determine the kind and extent of $VF_6$ octahedral distortion with its apparent effect on the relative energies of the 3d electronic states; this would help to interpret magnetic properties of this and other trirutile compounds. Added inducements to determine the complete crystal structure were to verify the periodic ordering of $Li^+$ ions between pairs of vanadium ions along the tetragonal (crystallographic $c$) axis and to address the question of an ordered vs. a random (mixed-valent) arrangement of $V^{II}$ and $V^{III}$ species in the lattice.

## Experimental Section

The $LiV_2F_6$ sample was prepared by mixing 0.9313 g of LiF, 3.1933 g of $VF_2$, and 3.8754 g of $VF_3$, vacuum encapsulating inside a cylindrical 1.91 × 3.18 cm molybdenum container, sealing with an electron beam welder, and heating at 800 °C for 28 days inside an evacuated furnace tube of a Hevi-Duty Lindberg furnace. The product (a brownish red powder) was analyzed optically by both stereoscopic and polarized microscopy. Under magnification, the tiny crystals appeared brownish red to transmitted light, were highly birefringent, but were at least an order of magnitude more optically dense than the starting materials, $VF_2$ (blue) and $VF_3$ (green). Anal. Calcd for $LiV_2F_6$: Li, 3.12; V, 45.73; F, 51.16. Found: Li, 3.00; V, 45.48; F, 50.95.

A small crystal of approximate dimensions 0.25 × 0.25 × 0.25 mm was selected for X-ray diffraction investigation on an Enraf-Nonius CAD-4F automated diffractometer operating at room temperature and employing graphite-monochromatized Mo $K\alpha_1$ radiation ($\lambda$ = 0.709 26 Å).

(1) (a) The University of Mississippi. (b) Fairchild Industries.
(2) (a) W. H. Baur, *Acta Crystallogr.*, **9**, 515 (1956); (b) D. T. Cromer and K. Herrington, *J. Am. Chem. Soc.*, **77**, 4708 (1955).
(3) (a) J. W. Stout and W. O. J. Boo, *J. Appl. Phys.*, **37**, 966 (1966); (b) J. W. Stout and W. O. J. Boo, *J. Chem. Phys.*, **71**, 1 (1979).
(4) J. W. Stout and S. A. Reed, *J. Am. Chem. Soc.*, **76**, 5279 (1954).
(5) (a) K. H. Jack and R. Maitland, *Proc. Chem. Soc. London*, 232 (1957); (b) C. Billy and H. M. Haendler, *J. Am. Chem. Soc.*, **79**, 1049 (1957).
(6) J. B. Goodenough, "Magnetism and the Chemical Bond", Interscience, New York, 1963, pp 165–185.
(7) J. Kanamori, *J. Phys. Chem. Solids*, **10**, 87 (1959).
(8) J. W. Cable, M. K. Wilkinson, and E. O. Wollan, *Phys. Rev.*, **118**, 950 (1960).
(9) R. A. Erickson, *Phys. Rev.*, **90**, 779 (1953).
(10) (a) J. C. Taylor and P. W. Wilson, *J. Less-Common Met.*, **34**, 257 (1974); (b) P. Fischer, W. Haelg, D. Schwarzenbach, and H. Gamsjaeger, *J. Phys. Chem. Solids*, **35**, 1683 (1974).
(11) H. Y. Lau, J. W. Stout, W. C. Koehler, and H. R. Child, *J. Appl. Phys.*, **40**, 1136 (1969).
(12) R. F. Williamson and W. O. J. Boo, *Inorg. Chem.*, **19**, 31 (1980).
(13) O. von Heidenstam, *Ark. Kemi*, **28**, 375 (1967).
(14) (a) W. Viebahn, W. Rüdorff, and H. Kornelson, *Z. Naturforsch., B*, **22B**, 1218 (1967); (b) J. Portier, A. Tressaud, R. dePape, and P. Hagenmuller, *C. R. Hebd. Seances Acad. Sci., Ser. C.*, **267**, 1711 (1968); (c) W. Viebahn, W. Rüdorff, and R. Händler, *Chimia*, **23**, 503 (1969); (d) J. Portier, F. Menil, and A. Tressaud, *Mater. Res. Bull.*, **5**, 503 (1970); (e) W. Viebahn, and P. Epple, *Z. Anorg. Allg. Chem.*, **427**, 45 (1976); (f) V. J. Gaile, W. Rüdorff, and W. Viebahn, *Z. Anorg. Allg. Chem.*, **430**, 161 (1977).

0020-1669/83/1322-1060$01.50/0 

**Table I.** Atomic Parameters

| atom | Wyckoff position (site symm) | x/a | y/b | z/c | $U_{11}$[a] | $U_{22}$ | $U_{33}$ | $U_{12}$ | $U_{13}$ | $U_{23}$ |
|---|---|---|---|---|---|---|---|---|---|---|
| V | 4e (*mm*2) ($C_{2v}$) | 0 | 0 | 0.33263 (8) | 0.0073 (4) | 0 | 0.0052 (3) | −0.0005 (3) | 0 | 0 |
| F1 | 4f (*mm*2) ($C_{2v}$) | 0.3094 (11) | 0.3094 | 0 | 0.011 (2) | 0 | 0.018 (1) | −0.005 (1) | 0 | 0 |
| F2 | 8j (*m*) ($C_s$) | 0.2971 (9) | 0.2971 | 0.3277 (2) | 0.015 (1) | 0 | 0.0103 (9) | −0.001 (1) | −0.002 (1) | 0 |
| Li | 2a (*mmm*) ($D_{2h}$) | 0 | 0 | 0 | 2.0 (3)[b] | 0 | 0 | 0 | 0 | 0 |

[a] The form of the anisotropic thermal factor is $\exp[-2\pi^2(a^{*2}U_{11}h^2 + \ldots + 2a^*b^*U_{12}hk + \ldots)]$. [b] Isotropic temperature factor.

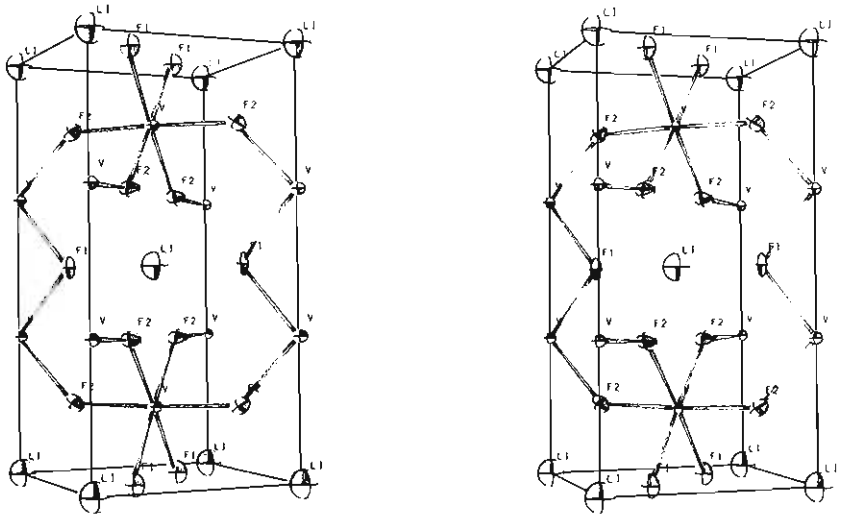

**Figure 1.** Stereoscopic projection of $LiV_2F_6$ showing unit cell contents.

The unit cell constants, based on a least-squares fit to the setting angles for 25 reflections, are $a = 4.697$ (3) Å, $b = 4.697$ (3) Å, $c = 9.289$ (3) Å, $\alpha = \beta = \gamma = 90°$, $d_{calcd} = 3.610$ g cm$^{-3}$ for $Z = 2$ (formula unit $LiV_2F_6$; formula weight 222.82), $d_{obsd} = 3.68$ (5) g cm$^{-3}$ (pycnometry), and $\mu = 48.82$ cm$^{-1}$. The unit cell data are in excellent agreement with previously published values.[12] The observed systematic absences [$(0kl)$, $k + l = 2n + 1$] are consistent with three tetragonal space groups: $P4_2/mnm$ ($D_{4h}^{14}$), $P\bar{4}n2$ ($D_{2d}^{8}$), and $P4_2nm$ ($C_{4v}^{4}$). Of these, the calculated structure could be refined only in space group $P4_2/mnm$, as discussed below.

Intensity data were collected with the diffractometer operating in the bisecting geometry mode, and employing the $\theta$–$2\theta$ scan technique. A set of 568 unique reflections were surveyed of which 371 had $I_{obsd} > 3\sigma(I_{obsd})$ and were subsequently used in the structure refinement.

The structure solution and refinement were carried out on a PDP1134 computer using the SDP (structure determination package) set of programs written by Frenz.[15] The X-ray atomic scattering factors used are those from ref 16. From the raw intensities ($I_{raw}$) the observed intensities ($F_o^2$) were obtained from Wilson plots; the estimated standard deviations, $\sigma(F_o^2)$, were obtained from the formula

$$\sigma(F_o^2) = [\sigma^2(I_{raw}) + (0.05I_{raw})^2]^{1/2}/Lp$$

where $Lp$ is the factor that corrects for Lorentz and polarization effects.

A trial structure based on the literature model structure of trirutile[17] was refined by full-matrix least squares [including positional parameters, isotropic (Li) and anisotropic (V, F) thermal parameters, a secondary extinction parameter ($g = 5.98 \times 10^{-5}$), and an overall scale factor] to convergence in the space group $P4_2/mnm$. The discrepancy factors based on the final parameters are $R = \sum(|F_o| - |F_c|)/\sum|F_o| = 0.050$ and $R_w = [\sum w(|F_o| - |F_c|)^2/\sum|F_o|^2]^{1/2} = 0.087$, where $w = 4F_o^2/\sigma^2(F_o^2)$; the goodness-of-fit value is $E = [\sum w(|F_o| - |F_c|)^2/(NO - NV)]^{1/2} = 2.891$, where NO = the number of observations = 371 and NV = the number of parameters = 17. Refinements using ionic scattering factors (for $V^{2+}$, $V^{3+}$, and $F^-$)[16] yielded no significant improvement. The final difference Fourier revealed two spurious peaks, of height 1.5 e Å$^{-3}$, at ($^1/_4$, $^1/_4$, $^1/_2$) and at (0.19, 0.19, 0.13). Attempts to refine the structure in space groups $P\bar{4}n2$ and $P4_2nm$ failed.

The final positional and thermal parameters are listed in Table I. The unit cell contents are shown in Figure 1. Table II gives the interatomic distances, and Table III lists the interatomic angles. The

**Table II.** Interatomic Distances (Å)

| | | | |
|---|---|---|---|
| Li-V | 3.090 (0) | $F1-F1^1$ | 2.532 (5) |
| V-V | 3.109 (1) | F1-F2 | |
| $V-V^1$ | 3.659 (1) | $F1^1$-F2 | 2.839 (3) |
| V-F1 | 2.005 (1) | F1-$F2^1$ | |
| $V-F1^1$ | | F1-$F2^3$ | 3.045 (1) |
| V-F2 | 1.975 (2) | $F1^1-F2^2$ | |
| $V-F2^1$ | | $F1^2-F2^2$ | |
| $V-F2^2$ | 2.008 (2) | $F1^2-F2^3$ | |
| $V-F2^3$ | | $F1^2-F2^4$ | 2.933 (3) |
| $Li-F1^2$ | 2.056 (2) | $F1^2-F2^5$ | |
| $Li-F1^3$ | | $F1^3-F2^3$ | |
| $Li-F2^2$ | | $F1^3-F2^5$ | |
| $Li-F2^3$ | 2.093 (2) | $F2-F2^2$ | |
| $Li-F2^4$ | | $F2-F2^3$ | 2.792 (1) |
| $Li-F2^5$ | | $F2^1-F2^3$ | |
| | | $F2^2-F2^3$ | 2.695 (4) |
| | | $F2^4-F2^5$ | |

**Table III.** Angles between Interatomic Vectors (deg)

| | | | |
|---|---|---|---|
| $F1-V-F1^1$ | 78.31 (10) | $F1^2-Li-F1^3$ | 179.97 (07) |
| F1-V-F2 | 91.03 (09) | $F1^2-Li-F2^2$ | 90.00 (06) |
| $F1-V-F2^1$ | 91.03 (09) | $F1^2-Li-F2^3$ | 90.00 (06) |
| $F1-V-F2^2$ | 177.01 (06) | $F1^2-Li-F2^4$ | 90.00 (06) |
| $F1-V-F2^3$ | 98.69 (08) | $F1^2-Li-F2^5$ | 90.00 (06) |
| $F1^1-V-F2$ | 91.03 (09) | $F1^3-Li-F2^2$ | 90.00 (06) |
| $F1^1-V-F2^1$ | 91.03 (09) | $F1^3-Li-F2^3$ | 90.00 (06) |
| $F1^1-V-F2^2$ | 98.69 (08) | $F1^2-Li-F2^4$ | 90.00 (06) |
| $F1^1-V-F2^3$ | 177.01 (06) | $F1^2-Li-F2^5$ | 180.00 (13) |
| $F2-V-F2^1$ | 177.31 (08) | $F2^2-Li-F2^3$ | 80.18 (10) |
| $F2-V-F2^2$ | 89.01 (10) | $F2^2-Li-F2^4$ | 99.82 (10) |
| $F2-V-F2^3$ | 89.01 (10) | $F2^2-Li-F2^5$ | 90.00 (06) |
| $F2^1-V-F2^2$ | 89.01 (10) | $F2^3-Li-F2^4$ | 180.00 (13) |
| $F2^1-V-F2^3$ | 89.01 (10) | $F2^3-Li-F2^5$ | 99.82 (10) |
| $F2^2-V-F2^3$ | 84.30 (09) | $F2^4-Li-F2^5$ | 80.18 (10) |

(15) B. Frenz, "SDP (Structure Determination Package) Version 16", Molecular Structure Corp., College Station, TX, 1979.
(16) J. A. Ibers and W. C. Hamilton, Eds., "International Tables for X-ray Crystallography", Vol. IV, Kynoch Press, Birmingham, England, 1976.
(17) A. F. Wells, "Structural Inorganic Chemistry", 3rd ed., Oxford Clarendon Press, Oxford, England, 1967, p 679.

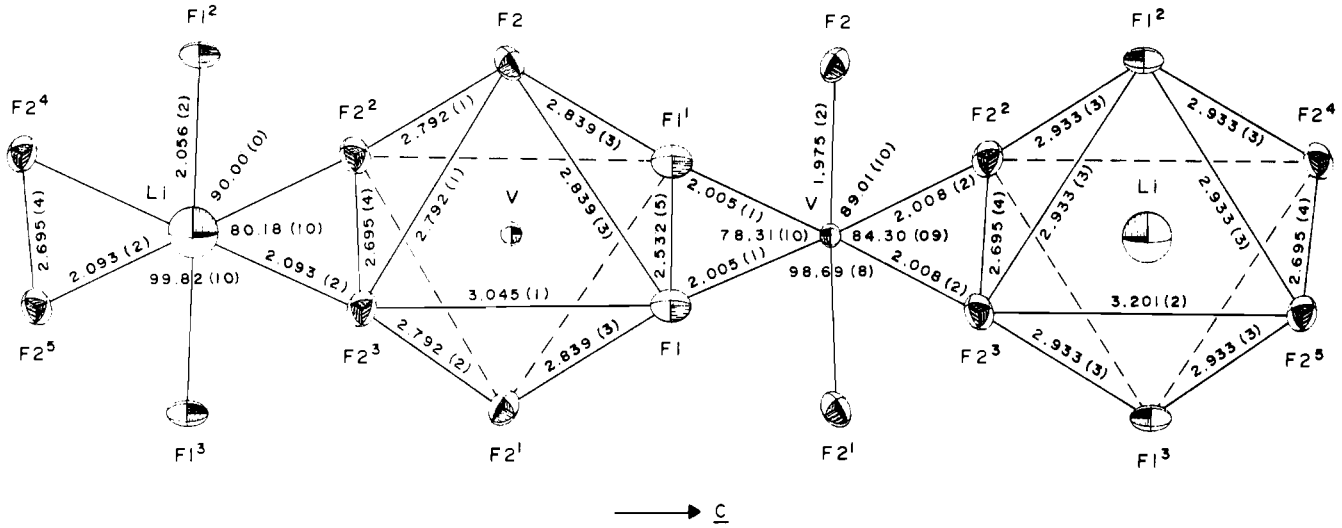


**Figure 2.** Chain of edge-sharing octahedra in $LiV_2F_6$ with relevant interatomic distances and angles.

chain of edge-sharing octahedra along the *c* axis is illustrated in Figure 2. Figures 1 and 2 were obtained with the computer program ORTEP[18] on a DEC 1077 computer.

The magnetic susceptibility was measured twice from 4.2 to 300 K on powder samples of mass 0.06596 and 0.06049 g. The results of the latter are illustrated as a plot of $\chi^{-1}$ vs. $T$ in Figure 3.

## Discussion

$LiV_2F_6$ crystallizes in the trirutile lattice ($P4_2/mnm$). There is only one crystallographic site for vanadium; hence, the $V^{2+}$ and $V^{3+}$ ions must randomly occupy the single 4e site; thus, $LiV_2F_6$ is a type III-A mixed-valence compound.[19] The color and optical density of $LiV_2F_6$ further support this claim. The coordination of $F^-$ ions around the V and Li sites is approximately octahedral. In $VF_2$, the nearest neighboring V ions form linear chains along the *c* axis, but in $LiV_2F_6$ the chains are interrupted by $Li^+$ ions leaving only pairs of nearest neighboring V ions. These pairs have edge-sharing octahedra.

The coordination and principal octahedra are shown in Figure 2. Nearest neighboring V ions are 3.109 Å apart and second nearest neighbors are 3.6595 Å apart, as opposed to 3.2469 (10) and 3.761 (1) Å,[20] respectively, in $VF_2$, and nearest-neighbor distance of 2.633 Å[21] in bulk V metal. The V–F distances of 1.975, 2.005, and 2.008 Å are shorter than the corresponding distances in $VF_2$ (which are 2.073, 2.092, and 2.092, respectively).[20] All of the shorter distances in $LiV_2F_6$ are to be expected from the increased average valency of V and from the presence of the $Li^+$ ion in the lattice.

It is noteworthy that in $LiV_2F_6$, as in $VF_2$, the apical cation to anion distance is shorter (axially compressed) than the four equatorial cation–anion distances. In $LiV_2F_6$, there are two fluorine positions, designated F1 and F2 in Figure 1. The Li–F distances 2.056 Å (two) and 2.093 Å (four) are considerably larger than the V–F distances. This is reflected by the $x/a$ and $y/a$ parameters that are 0.3094 and 0.2971 for F1 and F2, respectively. The difference in these values is too large to describe[14b] the fluorine atomic positions by a single parameter ($u$) as in the rutile structure. The $u$ value for $VF_2$ is reported to be 0.3055.[20] The F1 atoms, which are located

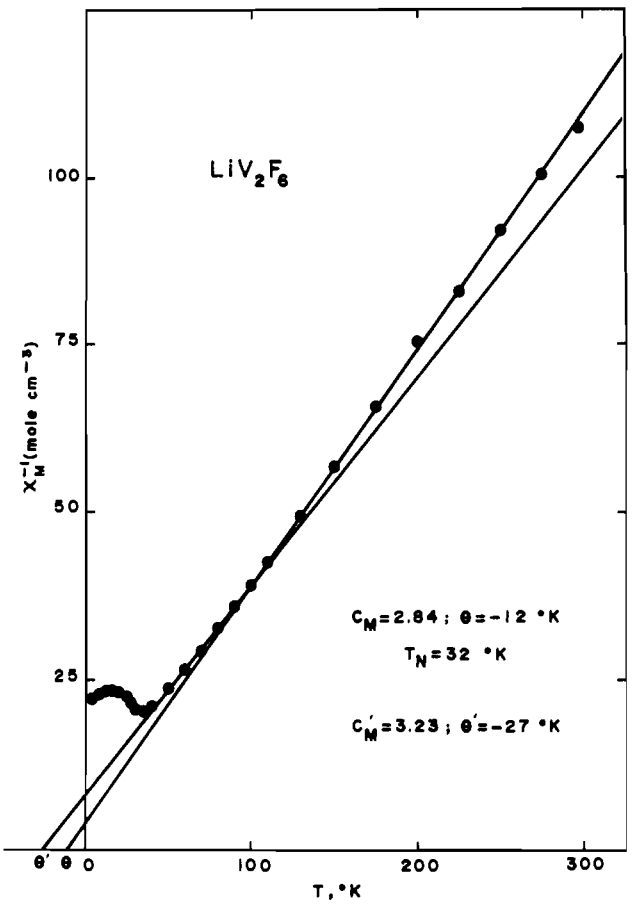


**Figure 3.** Inverse magnetic susceptibility vs. temperature of $LiV_2F_6$.

on Wyckoff 4f sites, have point group symmetry $mm2$ ($C_{2v}$), and F2 atoms located on 8j sites have symmetry $m$ ($C_s$). The thermal ellipsoids shown in Figure 1 indicate that F2 fluorine atoms are vibrating mainly perpendicular to the plane formed by the three M–F bonds. This is similar to the thermal anisotropy of fluorine atoms in $VF_2$ as well as other fluorides having the rutile structure, which are located on 4f sites. The thermal ellipsoids of the F1 atoms, however, vibrate mainly along the *c* axis, which is a characteristic that sets trirutile apart from rutile. By assuming a $F^-$ radius of 1.300 Å[22] in

(18) C. K. Johnson, "ORTEP II, A Fortran Ellipsoid Plot Program for Crystal Structure Illustration", Report ORNL-5138, Oak Ridge National Laboratory, Oak Ridge, TN, 1977.
(19) M. B. Robin and P. Day, *Adv. Inorg. Chem. Radiochem.*, **10**, 247 (1967).
(20) W. H. Bauer, S. Guggenheim, and J. C. Lin, *Acta Crystallogr., Sect. B*, **B38**, 351 (1982).
(21) J. D. H. Donnay, W. P. Mason, and E. A. Wood, "American Institute of Physics Handbook", 3rd ed., D. E. Gray, Ed., McGraw-Hill, New York, 1972, Chapter 9, p 7.
(22) R. D. Shannon and C. T. Prewitt, *Acta Crystallogr., Sect. B*, **B25**, 925 (1969).

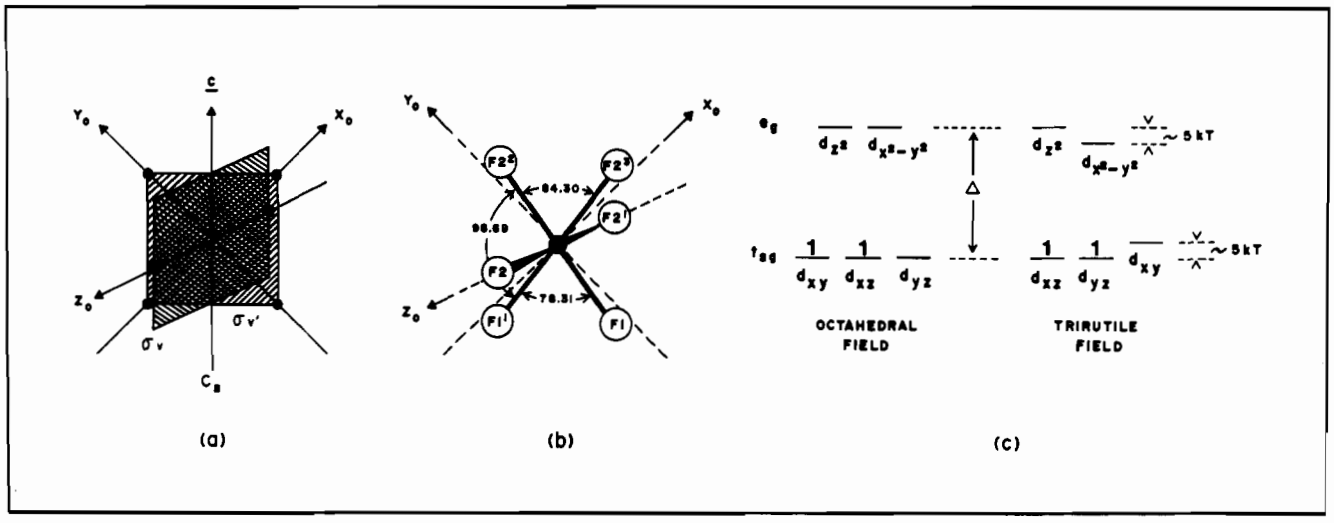


**Figure 4.** (a) Local Coordinate system ($x_0$, $y_0$, $z_0$) for a $VF_6$ octahedron, showing symmetry elements for the $C_{2v}$ point group. (b) Rutile distortion of $VF_6$ octahedron. (c) Effect of rutile distortion on the 3d energy states of vanadium.

3-fold coordination, one calculates an average V radius of 0.696 Å in $LiV_2F_6$, whereas in $VF_2$ the $V^{2+}$ radius is 0.784 Å.[20]

The coordination octahedra are somewhat distorted, typical of the rutile structure. The V–F–V bond angles between nearest and second nearest neighbors (Figure 2) are 101.69 (10) and 133.49 (7)°, which are not significantly different from those in $VF_2$ (101.79 and 129.11°). If one neglects the small differences in V–F distances (1.975, 2.005, and 2.008 Å), then the dominant distortion is an angular one. The point group symmetry of the $VF_6$ octahedra is in reality $mm2$ ($C_{2v}$). The $C_2$ axis lies parallel to the crystallographic $c$ axis but, unfortunately, is not along any V–F vector. For this reason, it is convenient to define a local coordinate system ($x_0$, $y_0$, $z_0$) for one of the $VF_6$ octahedra before introducing the "rutile" distortion (see Figure 4a). After the "rutile" distortion (Figure 4b), the $F1–V–F1^1$ bond angle is decreased from 90 to 78.31 (10)° and the $F1^1–V–F2^2$ angle is increased from 90 to 98.69 (8)°. This distortion will have an effect on the relative energies of the 3d electronic states. In the weak ligand field environment of the $F^-$ ions, the orthorhombic distortion of $LiV_2F_6$ can be qualitatively described as a "compression" of one of three $3d_{x_0y_0}$, $3d_{y_0z_0}$, or $3d_{z_0x_0}$ V atomic orbitals that belong to the $T_{2g}$ irreducible representation of the $O_h$ point group. From Figure 4b, it is clearly $d_{x_0y_0}$; hence, one could predict that this orbital would be slightly higher in energy than the degenerate pair $d_{y_0z_0}$, $d_{z_0x_0}$ (Figure 4c). By similar geometrical arguments, the $3d_{x_0^2-y_0^2}$ and $3d_{z_0^2}$ atomic orbitals, belonging to the $E_g$ irreducible representation of the $O_h$ point group, would be split into a higher energy state ($d_{z_0^2}$) and a lower one ($d_{x_0^2-y_0^2}$).

The energy separations [$\Delta(10Dq)$] of $E_g$ and $T_{2g}$ levels of divalent and trivalent first-row transition metal ions in fluoride octahedra are of the order of 50–100$kT$ (at 298 K). In crystal field language, this is explained as the energy difference between occupied 3d atomic orbitals that lie along interatomic M–F axes and undergo maximum Coulomb repulsion from the ligands (i.e., $d_{x^2-y^2}$ and $d_{z^2}$) and the occupied 3d atomic orbitals that lie between these axes (i.e., $d_{xy}$, $d_{yx}$, and $d_{zx}$). In $LiV_2F_6$, the angular distortion from octahedral symmetry (e.g., the $F1–F–F1^1$ bond angle is 78.31° and $F2^2–V–F2^3$ is 84.30° instead of 90°) should split the $T_{2g}$ and $E_g$ levels into sublevels differing in energy by $\sim 5kT$. If this interpretation is correct, the two 3d electrons of $V^{3+}$ should only populate the $d_{yz}$ and $d_{zx}$ orbitals and the orbital moment of $V^{3+}$ should be totally quenched at 298 K or below. The original magnetic susceptibility measurements on $LiV_2F_6$ did not confirm this effect.[12] The magnetic susceptibility has since been measured twice on recently prepared material, and the value $C_M$ = 2.84 was obtained from the paramagnetic region between 130 and 300 K. This compares favorably with a calculated "spin only" value, $C_M$ = 2.79. The repeated measurements also revealed a second paramagnetic region between 50 and 100 K (Figure 3). Although this may be accounted for by the high-temperature expansion of the susceptibility, another possible explanation for this phenomenon is that magnetic ordering occurs in two steps, as in $VF_2$. Near 100 K, short-range ordering between nearest neighbors would form ordered $V^{2+}–V^{3+}$ dimers. At lower temperatures ($T_N$ = 32 K) long-range three-dimensional ordering through second-nearest-neighbor interactions occurs. In the paramagnetic region, 50–100 K, a spin of $^5/_2$ would lead to the calculated value of $C_M'$ = 4.25. One can see, however, that the two $d_{x_0y_0}$ atomic orbitals of the $V^{2+}–V^{3+}$ dimer would be occupied by a single electron; hence, a small orbital moment should exist that would reduce $C_M'$ below the spin-only value. The observed value of $C_M'$ = 3.23 is qualitatively in agreement with this explanation. This value implies an average $g$ value of 1.72. Weiss constants obtained by extrapolation of the linear regions shown in Figure 3 give further insight into the magnetic interactions. The value $\Theta$ = −12 K indicates that both ferromagnetic and antiferromagnetic interactions are at work in $LiV_2F_6$. The value $\Theta'$ = −27 K supports the conclusion that second-nearest-neighbor interactions are antiferromagnetic. Interaction between nearest neighbors, therefore, must be ferromagnetic as was concluded earlier from the decision that the dimer has a spin of $^5/_2$.

**Table IV.** Madelung Energies for $LiV_2F_6$[a]

| charge distribution model | charges on V: at (0, 0, $z$) | at (0, 0, $\bar{z}$) | at ($^1/_2$, $^1/_2$, $^1/_2$ + $z$) | at ($^1/_2$, $^1/_2$, $^1/_2$ − $z$) | $E_M$, kJ/mol | $E_M$, eV/molecule |
|---|---|---|---|---|---|---|
| U | 2.5 | 2.5 | 2.5 | 2.5 | −10519.07 | −109.021 |
| A | 2.0 | 3.0 | 2.0 | 3.0 | −10685.85 | −110.750 |
| B | 3.0 | 3.0 | 2.0 | 2.0 | −10622.74 | −110.095 |

[a] The charges assumed for Li and F are 1+ and 1−, respectively.

The Madelung energy[23] was computed for $LiV_2F_6$ with the assumption of full charge transfer and uniform charges of 2.5 for all V ions (charge model U) and so-called Wigner lattice[24] disproportionated charges of 2+ and 3+ on the several V sites in the zeroth unit cell (charge models A and B). No

(23) R. M. Metzger, *Top. Curr. Phys.*, **26**, 80 (1981).
(24) E. Wigner, *Trans. Faraday Soc.*, **34**, 678 (1938).

"intramolecular" corrections were applied. The results given in Table IV favor, slightly, the Wigner lattice. The small energy margin by which the results differ is significant in that a mixed-valence state (U), if not the lowest energy state by the Madelung energy calculation (which always favors the disproportionated Wigner lattice A or B), can be stabilized by a strong electronic coupling between $V^{2+}$ and $V^{3+}$ along *c*.

## Conclusion

$LiV_2F_6$ is a mixed-valence salt that crystallizes in the trirutile (tapiolite) structure, space group $P4_2/mnm$. This structure exhibits pairs of crystallographically equivalent, orthorhombically distorted $VF_6$ octahedra that share one edge; the $VF_6$ pairs are separated along the tetragonal *c* axis by $LiF_6$ octahedra that share edges with the adjacent $VF_6$ octahedra.

The "rutile-type" distortion of $VF_6$ octahedra allows one to guess the 3d orbital occupancy in a weak-field scheme and to argue that the nearest-neighbor V–V interaction should be ferromagnetic and that the next-nearest-neighbor V–V interaction should be antiferromagnetic. Implicit in our argument is the assertion that angular distortion of ligands will have an effect on the mixing energy states.

The Madelung energy calculation favors, as expected, the non-mixed-valent Wigner crystal limit by an insignificant energy difference.

**Acknowledgment.** This research was supported by the National Science Foundation [Grants DMR 74-11970, 76-83360, 79-00313 (W.O.J.B.) and DMR 77-09314, 78-16998, 80-15658 (R.M.M.)] and the University of Mississippi. An electromagnet with power supply was provided by NASA Langley Research Center, and data reduction time was made available by the University of Mississippi Computer Center. The diffractometer and PDP 1134 computer were purchased by the State of Mississippi Building Commission.

**Registry No.** $LiV_2F_6$, 56092-96-7; V, 7440-62-2.

**Supplementary Material Available:** Tables of observed and calculated structure factor amplitudes (2 pages). Ordering information is given on any current masthead page.

---

Contribution from the Department of Chemistry, University of South Carolina, Columbia, South Carolina 29208

# Zirconium(IV) Poly(pyrazolyl)borate *tert*-Butoxide Derivatives. Stereochemically Nonrigid Six-Coordinate Molecules

DANIEL L. REGER* and MICHAEL E. TARQUINI

*Received August 23, 1982*

The complexes $[RB(pz)_3]Zr(O\text{-}t\text{-}Bu)Cl_2$ (R = *n*-Bu, *i*-Pr; pz = pyrazolyl ring) and $[HB(3,5\text{-}Me_2pz)_3]Zr(O\text{-}t\text{-}Bu)Cl_2$ have been prepared from the reaction of the previously reported $[RB(pz)_3]ZrCl_3$ complexes and 1 equiv of KO-*t*-Bu. $[i\text{-}PrB(pz)_3]Zr(O\text{-}t\text{-}Bu)_3$ and $[HB(3,5\text{-}Me_2pz)_3]Zr(O\text{-}t\text{-}Bu)_3$ are prepared with excess KO-*t*-Bu. The two insoluble complexes $[RB(pz)_3]ZrCl_3$ (R = H, pz) have been prepared free of $ZrCl_4$ for the first time and were characterized as their soluble $[RB(pz)_3]Zr(O\text{-}t\text{-}Bu)Cl_2$ derivatives. The complex $[HB(3,5\text{-}Me_2pz)_3]Zr(O\text{-}t\text{-}Bu)Cl_2$ shows the expected 2:1 pattern for each type of pyrazolyl reasonance in the $^1H$ and $^{13}C$ NMR spectra (one pz is trans to the O-*t*-Bu ligand, the other two are trans to Cl ligands). The other four $[RB(pz)_3]Zr(O\text{-}t\text{-}Bu)Cl_2$ complexes are fluxional at ambient temperature, but at low temperature limiting static spectra can be obtained. Careful investigation of the variable-temperature $^1H$ NMR spectra of $[B(pz)_4]Zr(O\text{-}t\text{-}Bu)Cl_2$ indicates that a mechanism involving a trigonal twist of the poly(pyrazolyl)borate ligand about the Zr–B axis can explain this dynamic behavior.

## Introduction

We have recently described the synthesis of $[RB(pz)_3]ZrCl_3$ (R = *n*-Bu, *i*-Pr; pz = pyrazolyl ring) and $[HB(3,5\text{-}Me_2pz)_3]ZrCl_3$,[1] the first well-characterized poly(pyrazolyl)borate complexes of zirconium.[2] Our choice of the alkyl-substituted $[RB(pz)_3]$ ligands was made to avoid potential steric problems offered by the $[HB(3,5\text{-}Me_2pz)_3]$ ligand and to ensure good solubility characteristics in standard organic solvents (complexes of $[HB(pz)_3]^-$ are frequently insoluble[4]). It is anticipated that these complexes represent the starting materials for an extensive series of derivatives of this early transition metal much in the same way that $Cp_2ZrCl_2$ and to a lesser extent $CpZrCl_3$ have been employed by others.[5]

To this end, we report here the synthesis and investigation of the fluxional behavior of a series of *tert*-butoxide derivatives of these poly(pyrazolyl)borate complexes. For complexes of the type $[RB(pz)_3]Zr(OR)Cl_2$, two of the pz rings are equivalent while the third is distinct. For the complexes of the $[HB(3,5\text{-}Me_2pz)_3]$ ligand, this nonequivalency is observed in both the $^1H$ and the $^{13}C$ NMR spectra at all temperatures studied. In contrast, the complexes of the $[RB(pz)_3]$ ligands display temperature-dependent $^1H$ and $^{13}C$ NMR spectra. We show that this fluxional behavior can be accounted for by a nondissociative trigonal-twist type mechanism.[6a] Although many stereochemically nonrigid molecules containing poly(pyrazolyl)borate ligands have been described,[6] these molecules

(1) Reger, D. L.; Tarquini, M. E. *Inorg. Chem.* **1982**, *21*, 840.
(2) A brief report[3] of $[B(pz)_4]_2ZrX_2$ (X = Cl, Br) and $[B(pz)_4]_4Zr$ has appeared. Following the preparations outlined in that publication, we have been unable to reproduce the reported NMR data.
(3) Asslani, S.; Rahbarnohi, R.; Wilson, B. L. *Inorg. Nucl. Chem. Lett.* **1979**, *15*, 59.
(4) McCleverty, J. A.; Seddon, D.; Bailey, N. A.; Walker, N. W. *J. Chem. Soc., Dalton Trans.* **1976**, 898.
(5) (a) Carr, D. B.; Schwartz, J. *J. Am. Chem. Soc.* **1979**, *101*, 3521. (b) Fachinetti, G.; Fochi, G.; Floriani, C. *J. Chem. Soc., Dalton Trans.* **1977**, 1946. (c) Wells, N. J.; Huffman, J. C.; Caulton, K. G. *J. Organomet. Chem.* **1981**, *213*, C17.
(6) (a) Meakin, P.; Trofimenko, S.; Jesson, J. P. *J. Am. Chem. Soc.* **1972**, *94*, 5677. (b) Manzer, L. E.; Meakin, P. Z. *Inorg. Chem.* **1976**, *15*, 3117. (c) Onishi, M.; Hiraki, K.; Shironita, M.; Yamaguchi, Y.; Nakagawa, S. *Bull. Chem. Soc. Jpn.* **1980**, *53*, 961. (d) Calderon, J. L.; Cotton, F. A.; Shaver, A. *J.Organomet. Chem.* **1972**, *37*, 127.

0020-1669/83/1322-1064$01.50/0 